

PAPER • OPEN ACCESS

Numerical prediction of Normal and Extreme Waves at Fukushima Offshore Site

To cite this article: Atsushi Yamaguchi and Takeshi Ishihara 2018 *J. Phys.: Conf. Ser.* **1037** 042022

View the [article online](#) for updates and enhancements.

Related content

- [Sound-Power Flow: Computed results compared with experimental data](#)
R Hickling
- [Ocean wave characteristic in the Sunda Strait using Wave Spectrum Model](#)
R Rachmayani, N S Ningsih, S R Adiprabowo et al.
- [Invited Article](#)
L H Ying, Z Zhuang, E J Heller et al.

Numerical prediction of Normal and Extreme Waves at Fukushima Offshore Site

Atsushi Yamaguchi¹ and Takeshi Ishihara²

¹Associate Professor, School of Engineering, The University of Tokyo

²Professor, School of Engineering, The University of Tokyo

E-mail: atsushi@bridge.t.u-tokyo.ac.jp

Abstract. In this study, wave hindcasting was performed at Fukushima floating offshore wind turbine demonstration site by using Wave Watch III, and the simulation results were validated by using measurement data. Following results were obtained. It was found that the use of the computational domain which covers whole the Pacific Ocean improves the prediction accuracy of significant wave height and wave period. By applying correction factors to the extreme value of the significant wave height results in the accurate estimation of the average value and the frequency distribution of the significant wave height. The long-term variations of the annual average significant wave height and period as well as the extreme value distribution of the annual maximum wave height are estimated from 10 years of hindcasting data. Gumbel fitting can be used for the estimation of the extreme wave height in tropical cyclone prone region. The relationship between extreme wave height and period is consistent with IEC61400-3. However, when all the event is included, the effect of the swell cannot be neglected and a model proposed by Goda should be used. A model to describe the joint probability distribution of wind speed, wave height and wave period is proposed. Predicted joint probability distribution based on this model shows good agreement with measurement.

1. Introduction

Estimation of the extreme wave height with the recurrence period of 50 years and the joint probability distribution of mean wind speed, significant wave height and peak wave period is needed for the design of offshore wind turbines. Hindcasting is typically used for the assessment of wave condition for offshore wind applications [1]. However, several problems are left to be solved.

First of all, along the Pacific coast of Japan, swell plays an important role and computational domain size needed to simulate the swell component is not clear. For example, it is expected that the swell caused by the wind far from the coastline of Japan, may affect the local sea condition, but there has been no guideline on the computation domain size needed to simulate the swell component.

Secondly, along the coastline of Japan, the tropical cyclone may play a significant role on the extreme wave height. In case of extreme wind estimation, Ishihara and Yamaguchi [2] showed



Gumbel fitting may cause large uncertainty and Monte Carlo simulation of tropical cyclone is needed to reduce the uncertainty, but the applicability of Gumbel distribution to the extreme wave distribution is not investigated. Further, in the swell prone region, the applicability of the relation between wave height and wave period specified in IEC61400-3 [3] may not be applicable and further analysis is needed.

Lastly, for the evaluation of joint probability distribution of wave height and wave period, typically, the result of the hindcasting is directly used, but this may result in non-smooth probability distribution which caused uncertainty in the fatigue load analysis and better method to estimate the probability distribution is needed.

This study focuses on these three points and proposes methods for the estimation of design wave condition of offshore wind farm along the coastline of Japan.

2. Wave hindcasting and validation at Fukushima site

In this study, metocean conditions measured in Fukushima Floating Offshore Wind Farm Demonstration (Fukushima FORWARD) Project[4] were used as validation data. In this project, a met mast of the height of 60m above sea level is installed on the substation floater together with Doppler lidar, wave meter is installed in the hull of the substation floater and wave buoy is installed in the same area. Statistical significant wave height ($H_{1/3}$) and significant wave period ($T_{1/3}$) are measured in this project. By cross-validating the wind speed, wave height and wave period, reliable dataset for one year was created and used in this study.

The third generation wave prediction model Wave Watch III ver 4.18[5]. was used for the hindcasting. Table 1 summarizes the computation domain and The surface wind data which is used as a boundary condition is obtained by mesoscale model WRF embedded in the global analysis data. Because the output of the wave prediction model is two directional wave spectrum model, significant wave height and significant wave period have to be calculated for the validation. In this study, following relationship relationships are assumed to calculate the statistical significant wave height and period from wave spectrum.

$$H_{1/3} = H_s = H_{m0} = 4\sqrt{m_0} \quad (1)$$

$$T_{1/3} = T_s = T_{m-1,0} = \frac{m_{-1}}{m_0} \quad (2)$$

Where m_n is the nth moment and defined by following equation.

$$m_n = \iint f^n E(f, \theta) df d\theta \quad (3)$$

Table 1 The computation domain of the hindcasting

	Domain 1	Domain 2	Domain 3	Domain 4
Computation period	From 1 Jan. 2006 to 31 Dec. 2015 (10 years)			
Horizontal resolution	0.5 degree	0.2 degree	0.05 degree	0.02 degree
Grid number	Case 1: 320×240 Case 2: 160×120	80×77	80×80	80×80
Bathymetry	ETOPO2			ETOPO1

Surface boundary condition (wind)	NCEP-FNL (1.0 degree)	WRF (18km)	WRF (6km)	WRF (2km)
Side boundary condition	Close	Nest-down (2 way)		
Resolution of spectrum	Frequency: 36(0.0345~0.97Hz), Direction 36			

Table 1 shows the four level nested grids used for the hindcasting. The effect of the computation domain was investigated by changing the size of the largest domain (domain 1), The grid interval of which is 0.5 degree both in latitude and longitude. Two different domain sizes were tested for domain 1: case 1 covers the entire Pacific Ocean and case 2 covers only north west part of the Pacific Ocean (Figure 1). Same computational domains are used for the domains 2, 3 and 4. One-year simulation for year 2015 was carried out and the simulation results were validated.

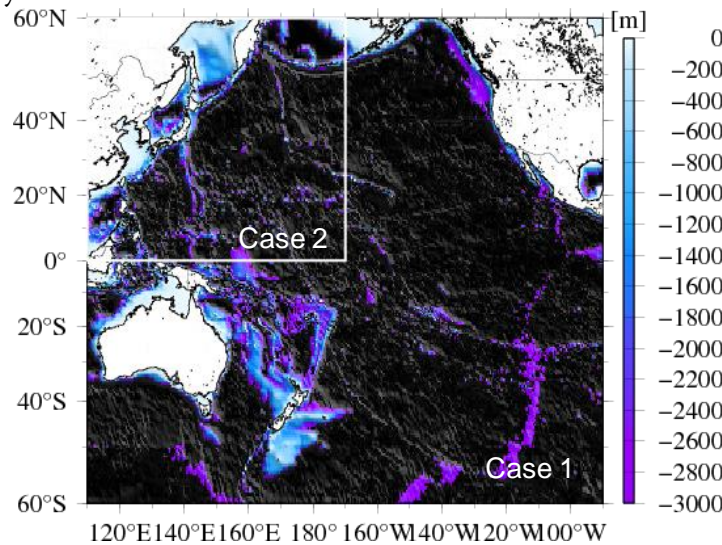


Figure 1 Two different computation domain 1: case 1 and case 2

The monthly averaged significant wave height and significant wave period are shown in figure 2 together with the measurement. When only north west Pacific is used for region 1 (case 2), the predicted significant wave periods are significantly smaller than the measurement while when the whole Pacific Ocean is covered in domain 1 (case 1), the underestimation of the significant wave period is improved and the predicted value shows better agreement with the measurement.

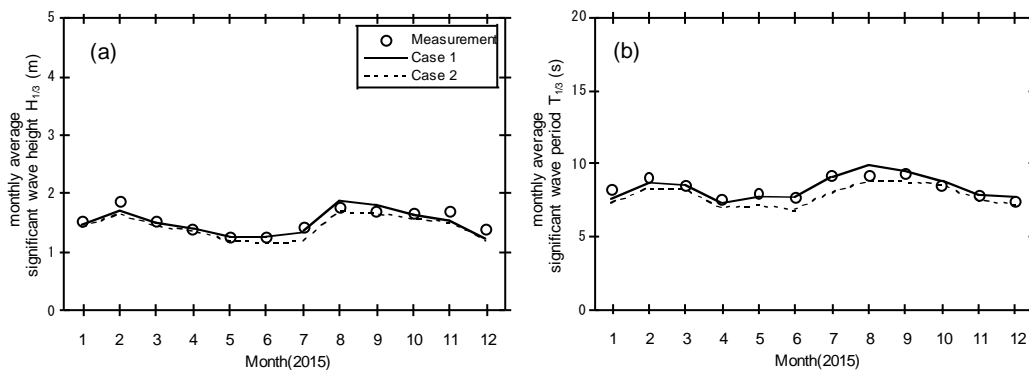


Figure 2 Simulated and measured monthly average significant wave height (a) and period (b)

By using the improved larger domain 1, the hindcasting was carried out for ten years, i.e., from January 2006 to December 2015. Because the wind speed used as the surface boundary condition has the averaging time of around three hours[6], the simulated wave height and period also has the evaluation time of around three hours (180 minutes). Yamaguchi and Ishihara[6] proposed a method to consider this difference, in which the relationship between the significant wave height with the evaluation time of M minutes and 20 minutes can be approximated by using following equation.

$$\frac{H_{1/3}^M}{H_{1/3}^{20}} = 1 - 0.05 \left(\frac{M - 20}{60} \right)^{0.3} \tag{4}$$

In this study, this equation is used to estimate the significant wave period with the evaluation time of 20 minutes ($H_{1/3}^{20}$) from that of 180 minutes ($H_{1/3}^{180}$). Then, a correction factor proposed by Mase et al.[7] is applied to estimate maximum significant wave period $H_{1/3}^{Max}$ by multiplying 1.19.

$$H_{1/3}^{Max} = 1.19H_{1/3}^{20} \tag{5}$$

These equations are applied when the peak wave height is predicted and within nine hours from the time when peak wave height is predicted, the wave height is linearly interpolated to have smooth change in the wave height. After this correction, predicted wave height show good agreement with the measurement. Figure 3 shows an example of the comparison of the predicted significant wave height before and after correction, predicted significant wave period and wave direction together with the measurement data.

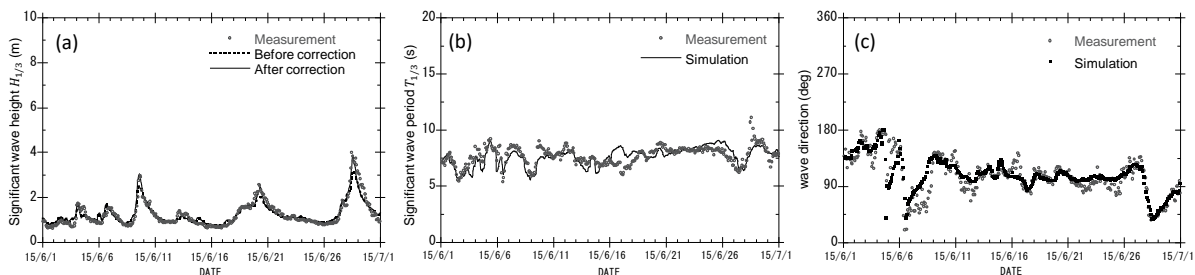


Figure 3 predicted and measured (a) significant wave height, (b) wave period and (c) wave direction

Figure 4 shows the monthly averaged significant wave height and wave period for all the months in year 2015. The frequency distribution of the wave height and period are also shown in figure 5. It is clearly shown that the predicted wave height and period show good agreements with measurement for all the month in year 2015.

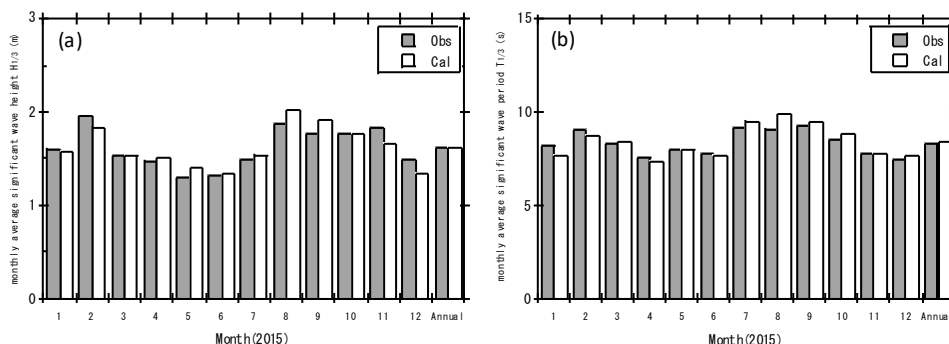


Figure 4 Monthly averaged significant wave height (a) and period (b)

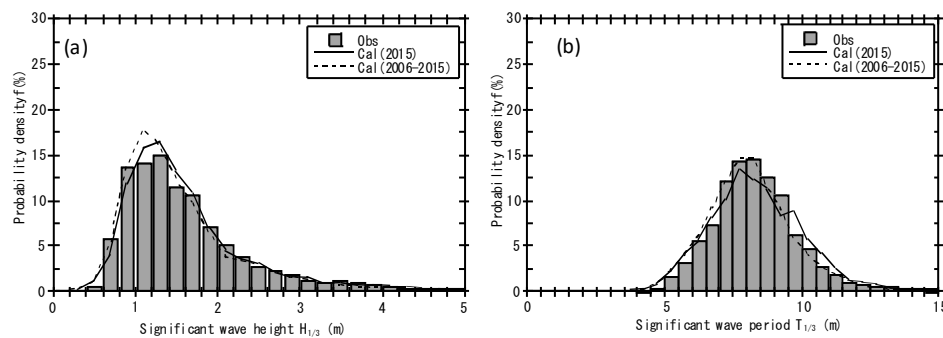


Figure 5 Frequency distribution of significant wave height (a) and period(b)

3. Estimation of the extreme wave height

By using 10 years of the hindcasting, after the correction of the peak value, the one year maximum significant wave height was extracted and reordered in ascending order, and frequency distribution of the extreme value are approximated by using Gumbel distribution. Moment method was used to estimate the parameters of the Gumbel distribution. Figure 6 (a) shows the estimated extreme wave height distribution with the uncertainty, together with the calculated annual maximum wave heights. The black circles show the extreme wave heights induced by tropical cyclones and the white circles shows those induced by other events. The uncertainty, or the dispersion of the Gumbel distribution can be calculated based on Gumbel theory as shown in equation (6).

$$\sigma_H^2 = \frac{\sigma_N^2}{N} [1 + 0.885(y - \gamma) + 0.6687(y - \gamma)^2] \quad (6)$$

It is shown that the Gumbel distribution can approximate the distribution and there seems no clear difference between the high wave event induced by tropical cyclones and the other events.

Figure 6 (b) shows the relationship between extreme wave height and wave period for the annual maximum wave height events. The relationship between wave height and period specified in IEC61400-3 is also shown in the figure. Most of the data are located within this range, but there are few exceptions. This is because the extreme wave events are caused by the local wind events and the effect of the swell is not significant. However, if all the events are included, the effect of the swell cannot be ignored and results shows larger variation. Figure 7 shows the relationship between significant wave height and period for all the events. Many data are located outside the region specified in IEC61400-3. This maybe the source of the uncertainty of the fatigue load assessment. A model proposed by Goda[8] is also shown in this figure. It is shown that for normal events, the model proposed by Goda should be used instead of the model specified in IEC61400-3.

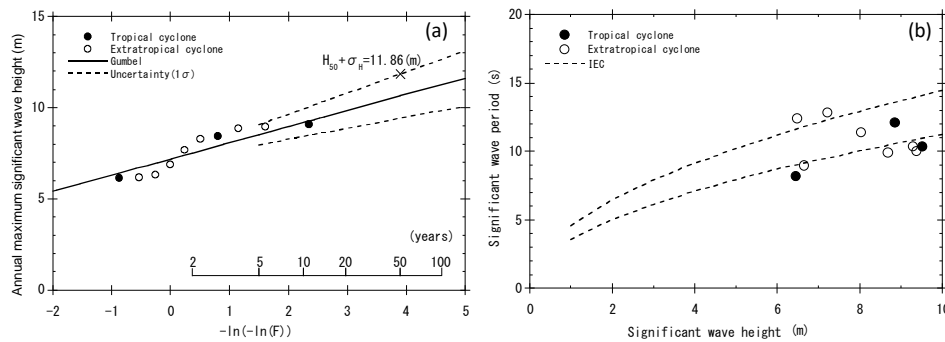


Figure 6 (a) Frequency distribution of the extreme wave height and (b) relationship between wave height and period for extreme wave height events

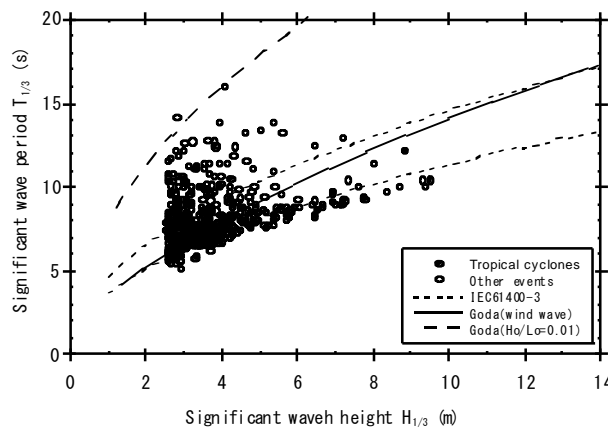


Figure 7 The relationship between wave height and period for all the events

Table 2 The model for the parameters of the probability distribution function of significant wave height and period

	Significant wave height	Significant wave period
mean	$\mu_{H_{1/3}} = \sqrt{\mu_{H_{1/3,W}}^2 + \mu_{H_{1/3,S}}^2}$ $\mu_{H_{1/3,W}} = \frac{0.30U_{10}^2}{g} \left[1 - \left\{ 1 + 0.004 \left(\frac{gF}{U_{10}^2} \right)^{1/2} \right\}^{-2} \right],$ $g = 9.81\text{m/s}^2 \quad F = 161,000\text{m}$ $\mu_{H_{1/3,S}} = (\mu_{H_{1/3}})_{0-1} = 1.31\text{m}$	$\mu_{T_{1/3}} = \frac{\mu_{T_{1/3,W}} \mu_{H_{1/3,W}}^2 + \mu_{T_{1/3,S}} \mu_{H_{1/3,S}}^2}{\mu_{H_{1/3,W}}^2 + \mu_{H_{1/3,S}}^2}$ $\mu_{T_{1/3,W}} = C_{T_{1/3,W}} \frac{2.74\pi U_{10}}{g} \left[1 - \left\{ 1 + 0.008 \left(\frac{gF}{U_{10}^2} \right)^{1/3} \right\}^{-5} \right]$ $C_{T_{1/3,W}} = 0.96 \quad g = 9.81\text{m/s}^2 \quad F = 161,000\text{m}$ $\mu_{T_{1/3,S}} = (\mu_{T_{1/3}})_{0-1} = 8.86\text{s}$
Standard deviation	$\sigma_{H_{1/3}} = \sqrt{\sigma_{H_{1/3,W}}^2 + \sigma_{H_{1/3,S}}^2}$ $\sigma_{H_{1/3,W}} = R_{H_{1/3,W}} \mu_{H_{1/3,W}}, \quad R_{H_{1/3,W}} = 0.36$ $\sigma_{H_{1/3,S}} = (\sigma_{H_{1/3}})_{0-1} = 0.52\text{m}$	$\sigma_{T_{1/3}} = \sqrt{\sigma_{T_{1/3,W}}^2 + \sigma_{T_{1/3,S}}^2}$ $\sigma_{T_{1/3,W}} = R_{T_{1/3,W}} \mu_{T_{1/3,W}}, \quad R_{T_{1/3,W}} = 0.14$ $\sigma_{T_{1/3,S}} = (\sigma_{T_{1/3}})_{0-1} = 1.34\text{s}$
Probability density	$f(H_{1/3}) = \frac{1}{\sqrt{2\pi} \zeta_{H_{1/3}} H_{1/3}} \exp \left[-\frac{1}{2} \left(\frac{\ln H_{1/3} - \lambda_{H_{1/3}}}{\zeta_{H_{1/3}}} \right)^2 \right]$ $\lambda_{H_{1/3}} = \ln \mu_{H_{1/3}} - \frac{1}{2} \zeta_{H_{1/3}}^2,$ $\zeta_{H_{1/3}}^2 = \ln \left[1 + \left(\frac{\sigma_{H_{1/3}}}{\mu_{H_{1/3}}} \right)^2 \right]$	$f(T_{1/3}) = \frac{1}{\sqrt{2\pi} \zeta_{T_{1/3}} T_{1/3}} \exp \left[-\frac{1}{2} \left(\frac{\ln T_{1/3} - \lambda_{T_{1/3}}}{\zeta_{T_{1/3}}} \right)^2 \right]$ $\lambda_{T_{1/3}} = \ln \mu_{T_{1/3}} - \frac{1}{2} \zeta_{T_{1/3}}^2, \quad \zeta_{T_{1/3}}^2 = \ln \left[1 + \left(\frac{\sigma_{T_{1/3}}}{\mu_{T_{1/3}}} \right)^2 \right]$

Correlation	$R_{H_{1/3}-T_{1/3}} = \tanh(\alpha U_{10} + \beta), \quad \alpha = 0.047\text{s/m}, \quad \beta = 0.278$
-------------	---

4. Estimation of joint probability distribution of wave height and wave period

For the fatigue load assessment of the offshore wind turbines, the joint probability distribution of wind speed, wave height and wave period is needed. In this study, the probability distribution of wave height and wave period is modelled by using log-normal distribution for each wind speed. Table 2 summarizes the model for the parameters of the probability distribution function of significant wave height and period and figure 8 shows the mean value and the standard deviation of the significant wave height and period as a function of wind speed. The examples of the distribution functions are shown in figure 9. The proposed model show good agreement with the distributions obtained from hindcasting.

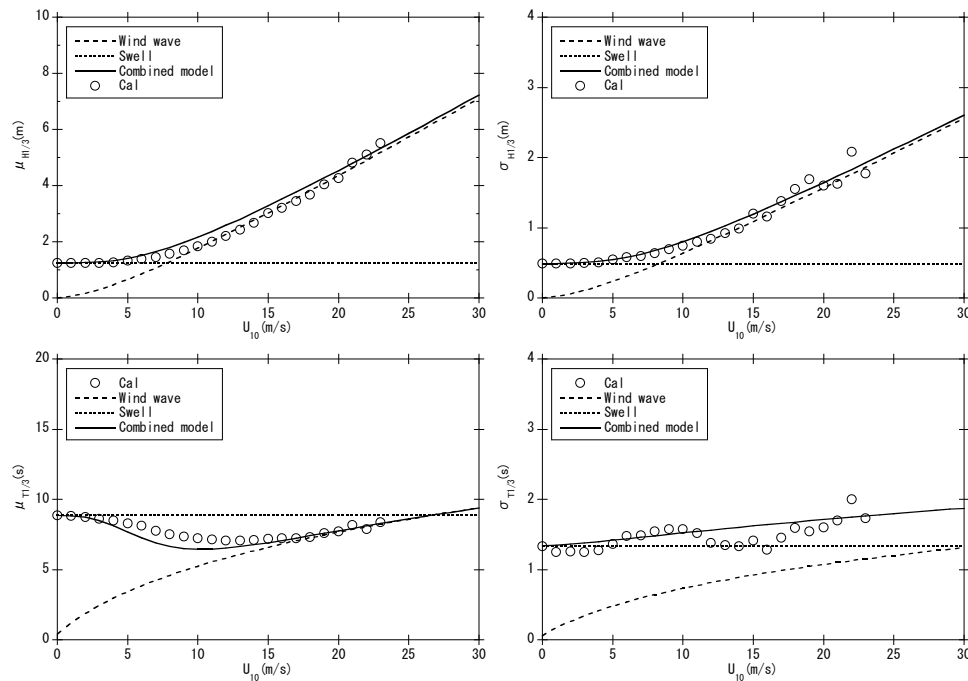


Figure 8 The mean value (a) and the standard deviation (b) of the significant wave height for different wind speed; the mean value (c) and the standard deviation (d) of the significant wave period for different wind speed

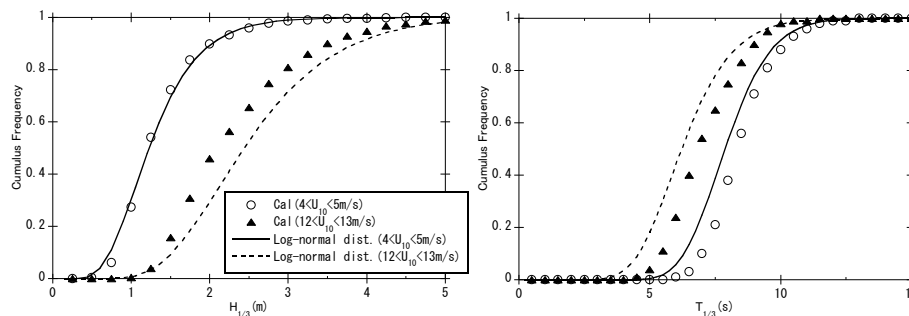


Figure 9 Examples of the frequency distribution of the significant wave height (a) and significant wave period (b)

In addition, the correlation between wave height and wave period is also modelled as a function of mean wind speed. This correlation is needed when Monte-Carlo simulation is performed to generate synthetic set of wind speed, wave height and wave period. Figure 10 shows the modelled correlation and the correlations obtained from hindcasting. Proposed model shows good agreement with the hindcasting.

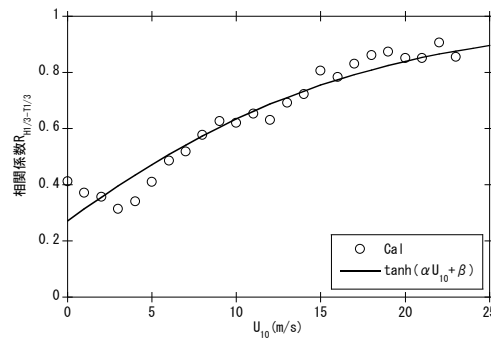


Figure 10 The correlation between significant wave height and period

Finally, based on these models, by using Monte-Carlo simulation, synthetic sets of mean wind speed, significant wave height and wave period were created. Figure 11 shows the joint probability distribution obtained by (a) measurement and (b) Monte-Carlo simulation. The estimated probability distribution by using Monte-Carlo simulation shows similar result with the measurement but smoother results with more data, which contribute to reduce the uncertainty of the fatigue load assessment.

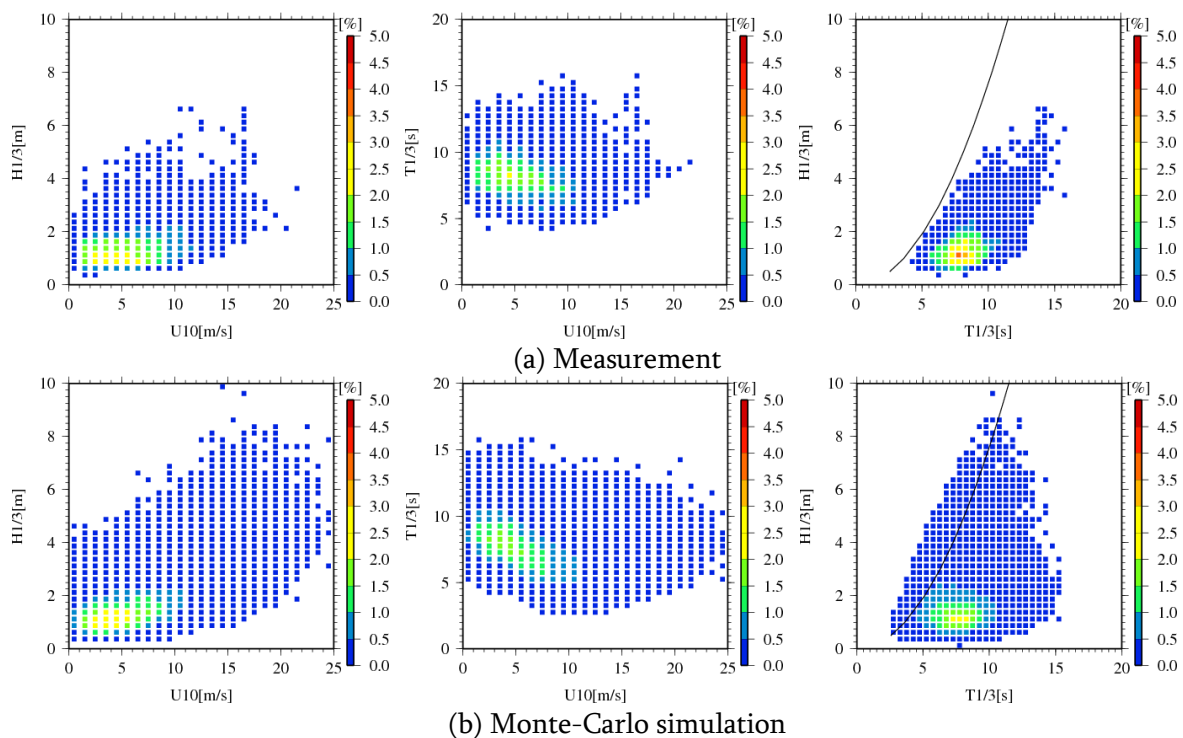


Figure 11 Measured and predicted joint probability distribution of wind speed, wave height and period

5. Conclusion

In this study, wave hindcasting was performed at Fukushima floating offshore wind turbine demonstration site by using Wave Watch III, and the simulation results were validated by using measurement data. Following results were obtained.

1. It was found that the use of the computational domain which covers whole the Pacific Ocean improves the prediction accuracy of significant wave height and wave period. By applying correction factors to the extreme value of the significant wave height results in the accurate estimation of the average value and the frequency distribution of the significant wave height.
2. The long-term variations of the annual average significant wave height and period as well as the extreme value distribution of the annual maximum wave height are estimated from 10 years of hindcasting data. Gumbel fitting can be used for the estimation of the extreme wave height in tropical cyclone prone region. The relationship between extreme wave height and period is consistent with IEC61400-3. However, when all the event is included, the effect of the swell cannot be neglected and a model proposed by Goda should be used.
3. A model to describe the joint probability distribution of wind speed, wave height and wave period is proposed. Predicted joint probability distribution based on this model shows good agreement with measurement.

Acknowledgement

This study was carried out as a part of Fukushima FORWARD project, funded by ministry of economy, trade and industry, Japan.

6. References

- [1] J.F.Manwell, C.N.Elkinton, A.L.Rogers and J.G.McGowan, Review of design conditions applicable to offshore wind energy systems in the United States, *Renewable and Sustainable Energy Reviews*, 11(2), 210-234, 2007
- [2] Takeshi ISHIIHARA, Atsushi YAMAGUCHI. Prediction of the extreme wind speed in the mixed climate region by using Monte Carlo simulation and Measure-Relate-Predict method, *Wind Energy*, 18(1): 171-186, 2015.
- [3] IEC61400-3, Wind Turbine - Part 3: Design requirements for offshore wind turbines, 2009.
- [4] A. Yamaguchi and T. Ishihara, Current status of research activity on floating offshore wind turbine in Japan, OFFSHORE2013, 2013.
- [5] Tolman H. L.: User manual and system documentation of WAVEWATCH III version 4.18. NOAA/NWS/NCEP/ MMAB Technical Note 316.,2014.
- [6] A. Yamaguchi and T. Ishihara, Effect of sampling time and disjunct sampling of significant wave height for the design of offshore wind farm, *Wind Energy Symposium*, Tokyo, 2012 (in Japanese).
- [7] H. Mase, N. Mori, T. Yasuda, J. Sakunaka and T. Utsunomiya, Assessment of Coastal Design Wave utilizing North Pacific Wave Analysis Data, *Jour. of JSCE*, Ser. B2 (Coastal Eng.), Vol.65, pp.146-150, 2009 (in Japanese)
- [8] Y.Goda: Random Seas and Design of Maritime Structures 3rd Edition, Advanced Series on Ocean Engineering, Vol.33, 2009.